24th COBEM - 2017

24th ABCM International Congress of Mechanical Engineering
December 3-8, 2017, Curitiba, PR, Brazil

COBEM-2017-1138
THERMO-HYDRAULIC CALCULATION IN CSP SYSTEMS USING THE FINITE VOLUME METHOD

Gabriel da Silva Lima
Gabriel Ivan Medina Tapia
Universidade Federal do Rio Grande do Norte, Departamento de Engenharia Mecânica, Laboratório de Sistemas Térmicos e Energias Alternativas - LSTEA, Campus Universitário, Lagoa Nova 59078970, Natal, RN, Brazil.
limagabriel@bct.ect.ufrn.br, gmedinat@ct.ufrn.br

Abstract. *In power generation projects whose energy supply comes from solar source it also becomes necessary to evaluate other parameters that are as important as the solar radiation so that it can make the process more efficient. This work aims to analyze the properties of the working fluid (water) in a power generation system whose energy input is made by heating the fluid by a Concentrating Solar Power (CSP) system of the Linear Fresnel Reflector type (LFR). Namely, in the LFR system a number of inclined flat mirrors redirects the Direct Normal Irradiance (DNI) to tubes, where the working fluid flows, that is located in the focus of the set of these mirrors. The mass, momentum and energy conservation equations were solved based on the Finite Volume Method (FVM), whose discretization was done by the upwind method and the pressure-velocity coupling problem will be solved by the SIMPLER method. Based on this method of resolution it was possible to obtain a monitoring of water status variables, such as pressure, temperature and title. A comparison was made between the numerical results and the experimental results found in the literature and an average relative error of approximately 3%.*

Keywords: *Concentrating Solar Power, Direct Normal Irradiance, Linear Fresnel Reflector, Finite Volume Method.*

1. INTRODUCTION

In recent years, on a global level, there has been growing concern about the environmental impacts of the most diverse types of conventional power plants. In the case of thermoelectric plants, for example, greenhouse gas emissions contribute to global warming. As a result, renewable energy sources emerge as options with low environmental impact.

In Brazil, because it has a large region with high incidence rates of solar radiation (Pereira *et al.*, 2017), analyzing the potential of this renewable source becomes strategic in order to provide its maximum use at a lower cost, based on the knowledge of all parameters involved in the power generation process.

In Concentrating Solar Power systems (CSP) the incident radiation, the Direct Normal Irradiance (DNI), is directed to absorbers located in the focus of the concentrators. These concentrators are mirrors that may have different formats. In Linear Fresnel Reflectors (LFR), flat mirrors are used, characterizing it as well as a low cost system compared to other types of systems (Canavarro, 2010).

With the objective of knowing the evolution of the change of the properties of the work fluid in a CSP system that uses LFR-type concentrators, a thermo-hydraulic calculation using the Finite Volumes Method (FVM) was developed in this work. It was adopted as Heat Transfer Fluid (HTF) the water. Sahoo *et al.* (2013) developed a similar work, however he used the finite difference method of first order to solve. Pye (2008) decides to focus the analysis on radiative heat exchange and states that only 10% of heat loss is due to convection and conduction mechanisms. For this work will be used the methodology implemented by Singh *et al.* (2010) for the calculation of the global coefficient of heat transmission using the correlations presented by Balaji and Venkateshan (1994).

In Figure 1 is shown the schematic drawing of the LFR system used for analysis. Note that the absorber tubes are contained in a trapezoidal cavity. The dimensions of this system are indicated in Tab. 1. For the validation of the method used, the temperature field along the length of the tube was compared with the results presented by Sahoo *et al.* (2012).

In the calculation implemented the following considerations were imposed:

- One-dimensional analysis;
- Uniform flow in fully developed regime;
- The heat flow is the same for all tubes;
- The heat flow between the tubes was neglected;
- Long and uninterrupted tubes;
- Constant properties within the subdomain of the control volume and approximated by the mean temperature and

pressure at the center of this subdomain;
- In the sub-cooling region an approximation was made using specific heats;
- The pipes are made of galvanized iron;
- The side and upper walls are insulated with glass wool;
- The bottom wall is made of simple glass.

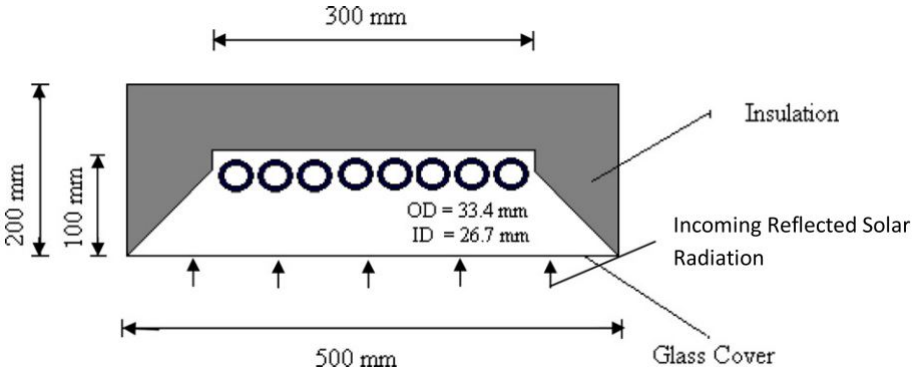

Figure 1. Schematic drawing of the LFR system, Sahoo *et al.* (2013).

Table 1. Specifications of the LFR system, Sahoo *et al.* (2012) and Sahoo *et al.* (2013).

Items	Dimensions
Bottom width of the cavity	500 mm
Top width of the cavity	300 mm
Side length of the cavity	141 mm
Depth of the cavity	100 mm
Number of tubes in the cavity	8
Absorber tube inner diameter	26.7 mm
Absorber tube outer diameter	33.4 mm
Absorber length	384 m
Number of reflector mirrors	8
Reflector width	1.8 m
Positions of reflectors from ground	1 m
Positions of cavity from the ground	13 m

2. METHODOLOGY

In order to obtain the water properties, it is necessary to solve the equations of conservation of mass, momentum and energy based on the FVM. According to Patankar (1980), this method, which is a variation of the Weighted Residues Method, the conservation equations are applied in differential form in subdomains of the mesh and then integrated throughout each control volume.

The discretization of the control volume was done by the upwind method. This method was used because it is relatively easy to implement and able to correctly identify the flow direction of the fluid, as opposed to the central difference method as mentioned by Patankar (1980) and Versteeg and Malalasekera (1995).

Due to the strong interaction between pressure and velocity, the SIMPLER method was used to receive the coupling problem. The SIMPLER method is the SIMPLE revised method (Patankar, 1980). Versteeg and Malalasekera (1995), using the Patankar (1980) approach, describes in a more understandable way and was therefore used as the main reference for the method.

The conservation equations of momentum and energy solved by the implemented method are shown in Eqs. (1), (2) and (3).

$$\frac{\partial}{\partial x}(\rho u u) = \frac{\partial}{\partial x}\left(\mu \frac{\partial u}{\partial x}\right) - \frac{\partial P}{\partial x} + S_u \tag{1}$$

$$S_u = \frac{\partial}{\partial x}\left(\mu \frac{\partial u}{\partial x}\right) \tag{2}$$

$$\dot{m}\left(h_I + \frac{u_I^2}{2}\right) + \dot{Q}_{in,CV} = \dot{m}\left(h_{I+1} + \frac{u_{I+1}^2}{2}\right) + \dot{Q}_{out,CV} \tag{3}$$

where u is the fluid velocity, μ is the dynamic viscosity, P is the fluid pressure, S_u is the source term calculated by Eq. (2), $\dot{m}$ is the water mass flow rate, h is the fluid enthalpy, $\dot{Q}_{in,CV}$ is the heat input in the control volume (CV) described by Eq. (4) and was adapted from Sahoo *et al.* (2013) and $\dot{Q}_{out,CV}$ is the heat output in the CV described by Eq. (5).

$$\dot{Q}_{in,CV} = \frac{DNI \cdot \rho_g \cdot (\sum A_r cos\,(\theta_n)) \cdot \gamma \cdot (\tau\alpha)}{n_t \cdot (N-1)} \tag{4}$$

where ρ_g is the reflectivity of mirrors, A_r is the reflection area of DNI, θ_n is the angle of inclination of the mirrors, γ is the solidity factor, $\tau\alpha$ is the product of transmissivity and absorptivity, n_t is the number of tubes within the cavity and N is the number of CV sub-domains.

$$\dot{Q}_{out,CV} = U \cdot A_{sup,CV} \cdot (T_{av,CV} - T_a) \tag{5}$$

where, U is the global coefficient of heat transfer, $A_{sup,CV}$ is the superficial area of the CV sub-domain, $T_{av,CV}$ is the average temperature in the center of sub-domain and T_a is the ambient temperature. In the calculation of U were considered the conduction in the tubes, convective and radiative effects within the cavity, conduction in the glass cover of the cavity and convective and radiative effects outside the cavity.

The global coefficient of heat transfer can be calculated by Eq. (6).

$$U = U_1 + U_2 \tag{6}$$

where,

$$U_1 = \frac{1}{\dfrac{1}{h_{cp} + h_{rp}} + \dfrac{A_p}{A_{cg}} \cdot \dfrac{1}{h_{co} + h_{ro}} + R_t + R_{cob}} \tag{7}$$

and

$$U_2 = \frac{1}{\dfrac{t_w}{k_{gw}} + R_t} \tag{8}$$

where h_{cp} and h_{rp} are, respectively, the convective and radiative coefficients of heat transfer inside the cavity, h_{co} and h_{ro} are, respectively, the convective and radiative coefficients of heat transfer out of the cavity, A_p is the project area of the absorbers pipe, A_{cg} is the area of the glass cover, R_t and R_{cob} are, respectively, the thermal resistances of conduction in the tube and the glass cover defined by Eqs. (9) and (10), t_w is the insulation thickness and k_{gw} is the thermal conductivity of the insulation.

$$R_t = \frac{1}{2} \cdot \frac{A_{sup,CV} \cdot ln\,(D_{ext}/D_{int})}{2\pi \cdot k_p \cdot \Delta x} \tag{9}$$

$$R_{cob} = \frac{t_{cob}}{k_g} \tag{10}$$

where D_{ext} and D_{int} are, respectively, the external and internal pipe diameters, k_p is the thermal conductivity of the pipe, Δx is the control volume length, t_{cob} is the glass cover thickness and k_g is the thermal conductivity of the glass cover.

The coefficients of heat transfer for convection and radiation inside the cavity can be calculated by the correlations presented by Balaji and Venkateshan (1994) and the coefficients of heat transfer for out of the cavity can be calculated by the methodology developed by Singh *et al.* (2010).

2.1 The pressure drop

The pressure drop for the single-phase region was calculated by Eq. (11).

$$\Delta P = f \cdot \frac{\Delta x}{D_{int}\rho} \cdot \frac{\dot{m}^2}{A_{int}^2} \tag{11}$$

where f is the friction factor, ρ is the specific mass, A_{int} is the cross-sectional area of the pipe.

For the two-phase region is added in the Eq. (11) the Friedel correlation used by Pye (2008).

3. RESULTS AND DISCUSSION

The entire calculation was implemented in Matlab R2016b and the HTF properties were obtained by the function Holmgren (2016). For validation purposes the obtained temperature field was compared with the results of Sahoo *et al.* (2012). For this was adopted an initial pressure of 45 bar, initial temperature of 37.5°C, DNI of 700 W/m^2 and mass flow rate of 0.15 kg/s. The comparison is shown in Fig. 2.

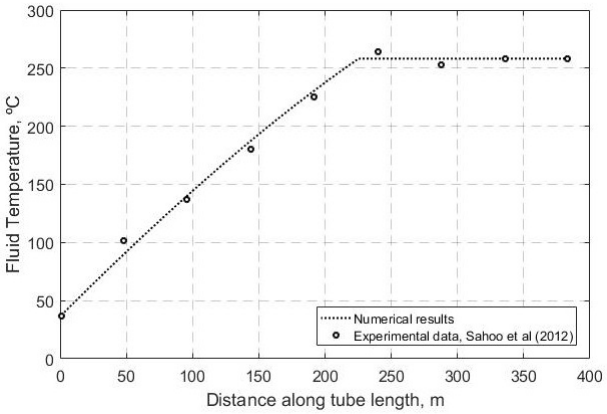

Figure 2. Comparison of the numerical method used with the results of Sahoo *et al.* (2012)

The average relative error between the proposed model and the data presented by Sahoo *et al.* (2012) was approximately 3% which indicates a good approximation between the numerical result and the experimental data. With the numeric method was achieved the saturation temperature of 258.2°C and Sahoo *et al.* (2012), 257.9°C.

For the other calculations it was adopted an initial pressure of 20 bar, initial temperature of 32°C, DNI of 700, 800 and 900 W/m^2 and mass flow rate of 0.15, 0.13 and 0.11 kg/s. The distribution of temperature and pressure, the pressure drop and the title along the flow were evaluated.

In the Figure 3 can be noted that the higher the DNI value the faster the approximate saturation temperature of 213°C. There was little variation in the saturation temperature for each DNI value, but with a maximum difference between them lower than 1°C.

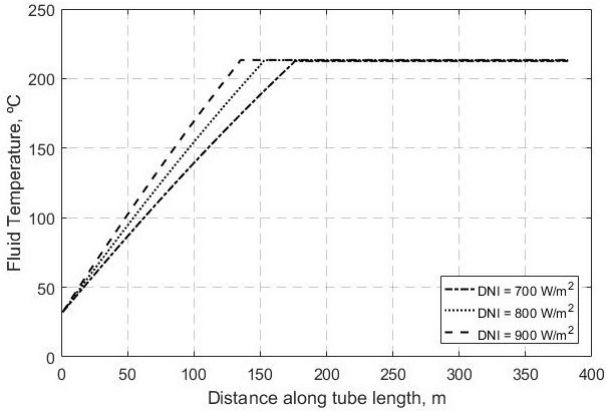

Figure 3. Fluid temperature distribution for different DNI values

In the Figures 4 and 5 may be noted that the higher the DNI value the faster the pressure fell in the two-phase region. In the single-phase region the pressure practically followed the same behavior. It is also noted that with each DNI increase there was an approximate increase of 0.1 bar in the drop of pressure at the exit of the flow.

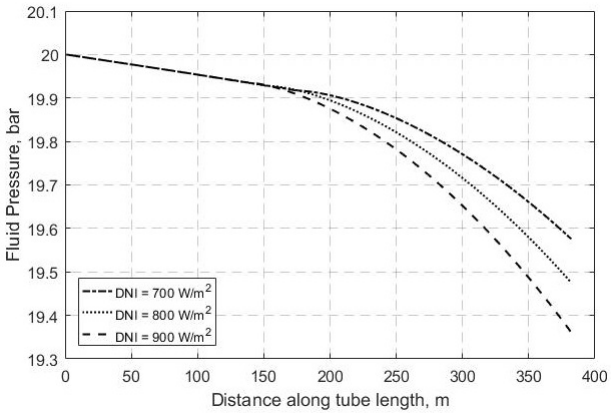

Figure 4. Distribution of fluid pressure along the flow to different DNI values

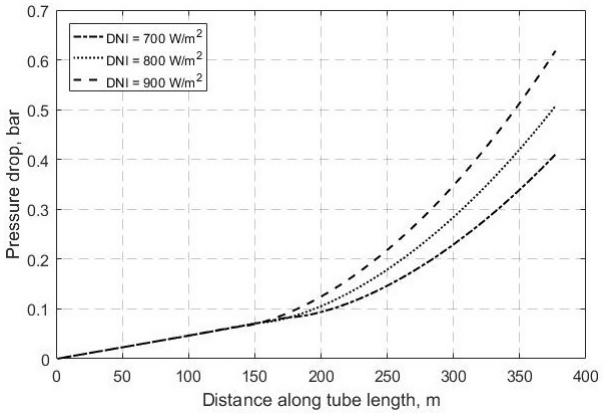

Figure 5. Distribution of pressure drop along the flow to different DNI values

In the Figure 6 can be noted that the higher the DNI value the greater the value of the title found ranging from approximately 0.45 for DNI of 700 W/m^2 up to approached 0.72 for DNI of 900 W/m^2.

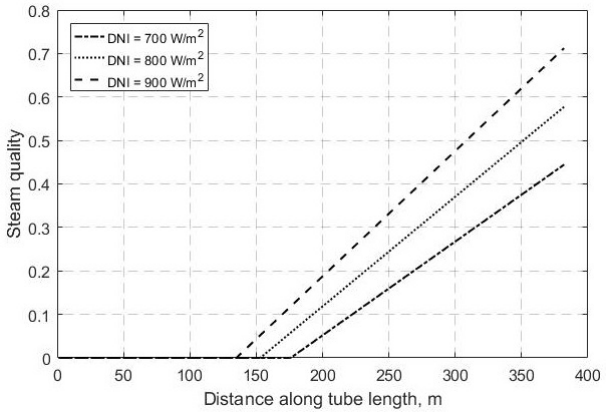

Figure 6. Change in steam quality for different DNI values

In order to evaluate the flow in relation to the mass flow change, the DNI value was set at 700 W/m^2.

In the Figure 7 a behavior similar to that of Fig. 3 for a same DNI value and varying only the mass flow rates of the fluid. It can be observed that the lower the flow rate, the faster the saturation region was reached.

In the Figures 8 and 9 may be noted that the lower the mass flow rate of the fluid, the lower the pressure drop at the outlet of the flow. For flow rate of 0.11 kg/s can see a pressure drop of 0.35 bar at the outlet. Differently from what happened with the DNI variation, when the DNI increase implied an increase in the pressure drop, with the decrease of the flow rate was verified a decrease of the pressure drop at the exit of the flow.

The behavior of the title change shown in Fig. 10 is similar to the behavior shown in Fig. 6. It can be seen that with decreasing flow rate, the higher the title achieved by a steam flow reaching the end of the flow approximately 0.74 to 0.11 kg/s, higher than the value obtained for DNI of 900 W/m^2 and with flow rate of 0.15 kg/s.

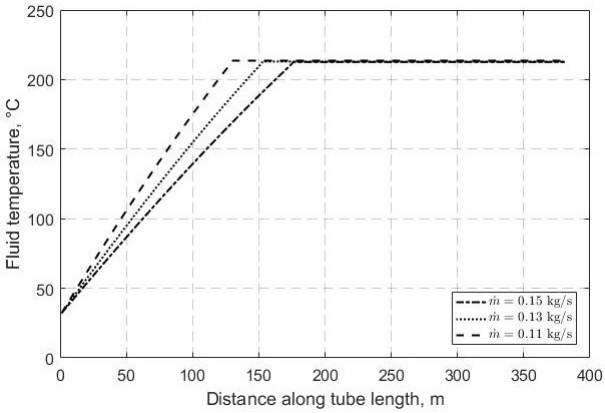

Figure 7. Distribution of fluid temperature for different mass flow rates and DNI of 700 W/m^2

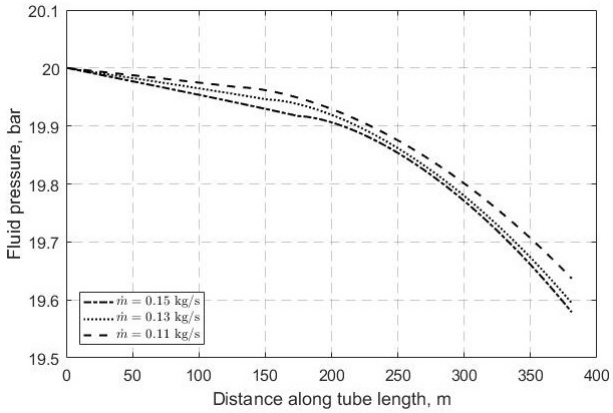

Figure 8. Distribution of fluid pressure of the fluid for different mass flows and DNI of 700 W/m^2

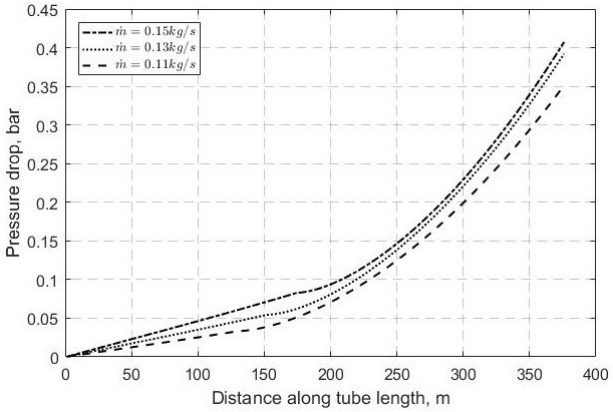

Figure 9. Distribution of pressure drop of the fluid for different mass flows and DNI of 700 W/m^2

3.1 Absorber Efficiency

The absorber efficiency can be calculated by Eq. (12), Sahoo *et al.* (2013).

$$\eta_{abs} = \frac{\dot{m} \cdot (h_N + u_N^2 - h_1 - u_1^2)}{\dot{Q}_{in}} \tag{12}$$

The Tables 2 and 3 shows the efficiency variation according to the parameter changes made above.

It can be seen from Tab. 2 that the increase in DNI implied higher efficiency within the values tested. And from Tab. 3 it can be seen that decreasing the mass flow resulted in lower efficiency within the values tested.

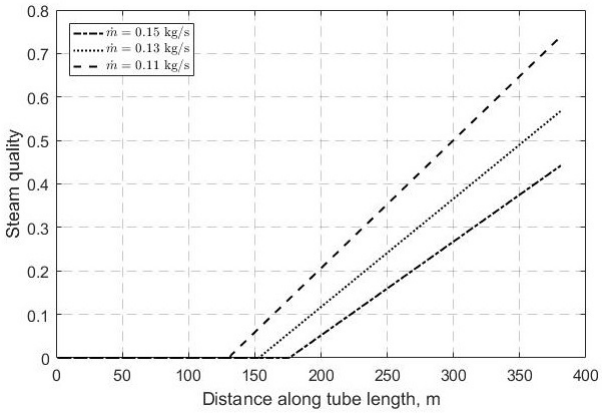

Figure 10. Change in steam quality for different flow rates and DNI of 700 W/m^2

Table 2. Absorber efficiency for different DNI

DNI	η_{abs}
700 W/m^2	0.884
800 W/m^2	0.894
900 W/m^2	0.903

Table 3. Absorber efficiency for different flow rates and DNI of 700 W/m^2

$\dot{m}$	η_{abs}
0.15 kg/s	0.884
0.13 kg/s	0.879
0.11 kg/s	0.874

4. CONCLUSIONS

In this work the properties of the HTF were estimated using the Finite Volumes Method. With this calculation it is possible to know better the evolution of the flow of the fluid besides to be able to know the quality of the exit steam for purposes of power production.

Comparing with data in the literature it was possible to obtain a very good approximation by validating the model and indicating that it has good predictive power over the calculated variables.

It was possible to observe that with the DNI increase the saturation region was started earlier and thus obtaining high quality steam at the end of the flow. It is also possible to verify that the increase in DNI implied both a drop in pressure and a absorber efficiency became higher.

With the change of mass flow, similar results were obtained in the evolution of temperature and title, however, it was verified that with the decrease of the flow both the pressure drop and the absorber efficiency became smaller.

For future work it is recommended to evaluate the distribution along the flow of HTF properties if another fluid were used in addition to studying other cavity formats. For this work, the analysis was made using LFR concentrators. Other types of concentrators may be used in the study.

5. ACKNOWLEDGEMENTS

The Laboratório de Sistemas Térmicos e Energias Alternativas team of the Universidade Federal do Rio Grande do Norte (LSTEA/UFRN) supported this work.

6. REFERENCES

Balaji, C. and Venkateshan, S.P., 1994. "Correlations for free convection and surface radiation in a square cavity". *Int J Heat Fluid Flow*, Vol. 15, No. 3, pp. 249–251.

Canavarro, D.C.d.S., 2010. *Modelização de campos de colectores solares lineares do tipo Fresnel; aplicação a um concentrador inovador do tipo CLFR*. Master's thesis, Universidade Técnica de Lisboa.

Holmgren, M., 2016. "X steam for matlab". 20 Apr. 2017 <https://www.x-eng.com>.

Patankar, S., 1980. *Numerical Heat Transfer and Fluid Flow*. Hemisphere Publishing Corporation, New York, 1st edition.

ISBN 978-0891165224 0.

Pereira, E.B., Martins, F.R., Gonçalves, A.R., Costa, R.S., Lima, F.J.L., Rüther, R., Abreu, S.L., Tiepolo, G.M., Pereira, S.V. and Souza, J.F., 2017. *Atlas Brasileiro Energia Solar*. INPE, São José dos Campos, Brasil, 2nd edition. ISBN 9788517000898.

Pye, J.D., 2008. *System Modelling of the Compact Linear Fresnel Reflector*. Ph.D. thesis, University of New South Wales.

Sahoo, S.S., Singh, S. and Banerjee, R., 2013. "Steady state hydrothermal analysis of the absorber tubes used in Linear Fresnel Reflector solar thermal system". *Solar Energy*, Vol. 87, No. 1, pp. 84–95. ISSN 0038092X.

Sahoo, S.S., Varghese, S.M. and Kumar, C.S., 2012. "Experimental investigation of convective flow boiling in the absorber tube of the linear Fresnel reflector solar thermal system". In *Solaris 2012*. Varanasi, India, February, pp. 1–8.

Singh, P.L., Sarviya, R.M. and Bhagoria, J.L., 2010. "Heat loss study of trapezoidal cavity absorbers for linear solar concentrating collector". *Energy Conversion and Management*, Vol. 51, No. 2, pp. 329–337. ISSN 01968904.

Versteeg, H.K. and Malalasekera, W., 1995. *An Introduction to Computational Fluid Dynamics: The Finite Volume Method*. Longman Scientific & Technical, New York, 1st edition.

7. RESPONSIBILITY NOTICE

The authors are the only responsible for the printed material included in this paper.